Nonlinear coupling in the crossing-angle beam-beam interaction

T. Chen
Stanford Linear Accelerator Center, Stanford University, Stanford, California 94309
(Received 8 March 1993; revised manuscript received 16 July 1993)

The effects of the beam-beam interaction with a small crossing angle on large-amplitude particles in an e^+e^- collider are studied. An analytical resonance analysis method is developed to understand the nonlinear coupling resonance driving mechanism. The major effect of the crossing angle for large-amplitude particles is to drive the $5Q_x \pm Q_s =$ integer resonance family. The analytic results are consistent with a computer simulation. The resonance is observed in the crossing-angle experiment in the Cornell Electron Storage Ring.

PACS number(s): 52.75.Di, 29.27.Bd, 41.75.Ht, 29.20.Dh

I. INTRODUCTION

To study *CP* violation in B-meson decays, a luminosity of at least 3×10^{33} $cm^{-2}sec^{-1}$ is needed, which is $\sim$10–50 times higher than what is currently achieved in electron-positron colliders. The most direct way to achieve the needed luminosity is to increase the collision frequency by shortening the space between bunches. This raises the problem of separating the bunches at the first parasitic collision point. One possible solution is to collide the beams with a crossing angle, and, in fact, proposed high-luminosity e^+e^- colliders either have a crossing angle or have a crossing angle as an option.

The introduction of a crossing angle in e^+e^- colliders causes nonlinear coupling between horizontal motion and longitudinal motion. This problem has been observed in operation [1] and discussed elsewhere [1–3]. This paper will concentrate on understanding the coupling resonance driving mechanism. In order to analyze the problem, we make a thin-lens approximation in which a particle gets only one momentum-changing kick when it passes the opposite bunch. This is a reasonable approximation being widely used in most beam-beam simulation programs, especially in the case of horizontal kick, where the change of beam size within one bunch length is not significant. The kick occurs when the particle passes the center of the opposing bunch. The strength of the kick, $\Delta r' = F(r)$, is a nonlinear function of the distance r between the particle and the center of the opposite bunch. In head-on collisions, r is the transverse displacement, and the kick is in the transverse plane, so that the process is nonlinear but not influenced by the longitudinal motion. In collisions with a crossing angle, however, r is a function of longitudinal displacement s and the crossing angle Φ, as well as transverse displacement. Figure 1 shows the geometry when the kick occurs with a crossing angle. The distance r between the test particle and the bunch center can be written as

$$r = x + s\tan\Phi \ . \tag{1}$$

The kick is a function of both transverse and longitudinal positions and, as a result, nonlinear synchro-betatron coupling is generated by the crossing-angle collision. In addition, the kick has a component in the longitudinal direction.

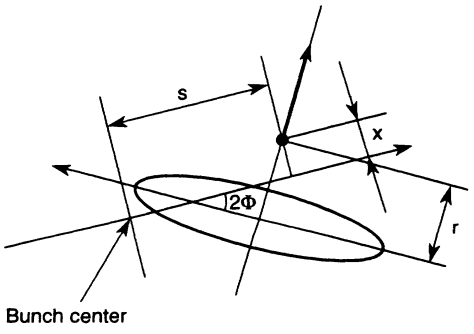

FIG. 1. Kick in crossing-angle collision.

This paper investigates the effects of the nonlinear coupling caused by the crossing-angle collision. Since another study suggests that the effects are mostly on the beam tail, rather than the beam core [3], the investigation is concentrated on large-amplitude particles. Another study [4] has investigated the crossing-angle beam-beam problem from the operational point of view. There are many measurements made in luminosity performance, beam-beam tune shift, etc.

The parameters used are based on the Cornell B-Factory (CESR-B) design, but the conclusion is general because the beam-beam interaction is essentially the same for all B-Factory designs. The experiment was performed on the Cornell Electron Storage Ring (CESR). The qualitative theoretical analysis, computer simulation, and experimental measurement are in agreement.

II. THEORETICAL ANALYSIS

A resonance analysis method is introduced in this section. The analysis is good for a linear storage ring with a single nonlinear thin elements [5], which is a reasonable approach to the beam-beam interaction problem. This method is developed to employ the Fourier transform to expand the nonlinear force, and relates the Fourier ex-

pansion components to certain resonances.

In an ideal storage ring, particles in each bunch are in three-dimensional oscillation about the center of the bunch. In the crossing-angle problem, we are interested in the horizontal (x) and longitudinal (s) motion. If we sit at one point of a linear ring observing a particle, its motion can be described by the difference equations:

$$x_{t+1}-2x_t\cos\mu_x+x_{t-1}=0\ , \tag{2}$$

$$s_{t+1}-2s_t\cos\mu_s+s_{t-1}=0\ , \tag{3}$$

where t stands for turn number and μ_x and μ_s are the whole-turn phase advances of the oscillations. It is straightforward to find their solutions:

$$x_t=A_x\cos(\mu_x t)\ , \tag{4}$$

$$s_t=A_s\cos(\mu_s t)\ . \tag{5}$$

With the crossing-angle collision, the difference equations become

$$x_{t+1}-2\cos\mu_x x_t+x_{t-1} =-\beta_x\sin\mu_x F(x_t+s_t\tan\Phi)\cos^2\Phi\ , \tag{6}$$

$$s_{t+1}-2\cos\mu_s s_t+s_{t-1} =\beta_s\sin\mu_s F(x_t+s_t\tan\Phi)\sin\Phi\cos\Phi \tag{7}$$

where F is the horizontal beam-beam kick, which can be approximated by a Dawson integral [6]:

$$F(r)=F_d\left[\frac{r}{\sqrt{2}\sigma_x}\right] \tag{8}$$

and

$$F_d(y)=e^{-y^2}\int_0^y e^{t^2}dt\ , \tag{9}$$

where σ_x is the horizontal beam size. β_s can be defined in an analogous way to the transverse motion [7]. In the difference equations (6) and (7), the kick modulation of the arrival time is neglected. This is because (1) the β_x at the interaction point (IP) is much larger than the bunch length. The β_x change in the bunch length range is negligible. (2) If the kick ($\Delta x'$) is transferred back to the IP through drift space, it has the same amount. For small crossing angle Φ, the nonlinear kick in the longitudinal plane is very weak. In addition, the longitudinal emittance is much larger than the horizontal emittance, which means s is much larger than x. Therefore the longitudinal nonlinear kick is negligible. Thus the above equations are simplified:

$$x_{t+1}-2\cos\mu_x x_t+x_{t-1} =-\beta_x\sin\mu_x F(x_t+s_t\tan\Phi)\cos^2\Phi\ , \tag{10}$$

$$s_{t+1}-2\cos\mu_s s_t+s_{t-1}=0\ . \tag{11}$$

Equation (11) has the same solution as (5). As the first step approximation, substitute (4) into the right-hand side of (10). Particles at large amplitude were used to evaluate the resonances, because previous studies have shown that crossing angles would mostly affect the large-amplitude particles [3]. 6σ amplitude is chosen because it is the typical amplitude for large-amplitude particles which we concentrate on, and changes near this amplitude do not change the qualitative conclusion. Taking $A_x=6\sigma_x$ and $A_s=6\sigma_s$, the Dawson integral becomes

$$F_d\left[\frac{6}{\sqrt{2}}\frac{\sigma_x\cos\mu_x t+\sigma_s\tan\Phi\cos\mu_s t}{\sigma_x}\right]\ . \tag{12}$$

From (12), we notice that the coupling term is actually proportional to $(A_s/\sigma_x)\tan\Phi$, rather than $\tan\Phi$. Since $A_s\sim\sigma_s$, the coupling generally scales as $(\sigma_s/\sigma_x)\tan\Phi$. This is called the normalized crossing angle.

Expanding the nonlinear kick in a two-dimensional Fourier series, the right-hand side of (10) can be written as

$$\tfrac{1}{2}\sum_{m,n}c_{m,n}\cos[(m\mu_x+n\mu_s)t]+d_{m,n}\cos[(m\mu_x-n\mu_s)t]\ . \tag{13}$$

Similarly, a solution is expected in the form

$$x_t=\tfrac{1}{2}\sum_{m,n}a_{m,n}\cos[(m\mu_x+n\mu_s)t] +b_{m,n}\cos[(m\mu_x-n\mu_s)t]\ . \tag{14}$$

Substituting the above equations into (10), it is easy to find the resonance driving relations:

$$a_{m,n}=\frac{c_{m,n}}{2\sin\frac{1}{2}[(m+1)\mu_x+n\mu_s]\sin\frac{1}{2}[(m-1)\mu_x+n\mu_s]}\ , \tag{15}$$

$$b_{m,n}=\frac{d_{m,n}}{2\sin\frac{1}{2}[(m+1)\mu_x-n\mu_s]\sin\frac{1}{2}[(m-1)\mu_x-n\mu_s]}\ . \tag{16}$$

Near resonances $(m\pm1)Q_x\pm nQ_s=$integer, the denominator is small. Then, $(a,b)_{m,n}$ has strong response to $(c,d)_{m,n}$. Therefore we can say that $c_{m,n}$ and $d_{m,n}$ drive these resonances.

Figure 2 shows the power spectrum of the Dawson integral (12), created by two-dimensional Fast Fourier transform (FFT). The power spectrum $\sqrt{c_{m,n}^2+d_{m,n}^2}$ gives the resonance driving strength. The phase of the driving terms is not important. Due to the symmetry of the function, the terms with $m+n=$even vanish. In the calculation, the crossing half angle Φ is 10 mrad. The beam sizes σ_x and σ_s are taken as 0.36 mm and 1 cm, respectively, corresponding to the CESR-B design. The normalized crossing angle, defined as $(\sigma_s/\sigma_x)\Phi$, is 0.278.

From Fig. 2, we can easily see that, besides the one-dimensional resonance driving terms ($n=0$), the strongest coupling resonance ($n\neq0$) driving terms are those with $m=4$, $n=1$ and $m=6$, $n=1$. According to the previous analysis, these two terms will drive $3Q_x\pm Q_s=$integer, $5Q_x\pm Q_s=$integer and $5Q_x\pm Q_s=$integer, $7Q_x\pm Q_s=$integer resonances, respectively. It is natural to conclude that the $5Q_x\pm Q_s=$integer reso-

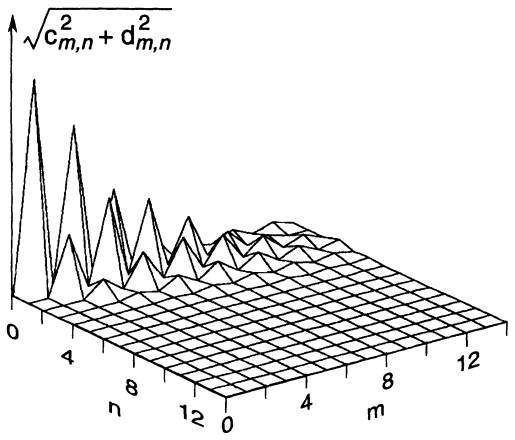

FIG. 2. The power spectrum of the crossing-angle beam-beam kick.

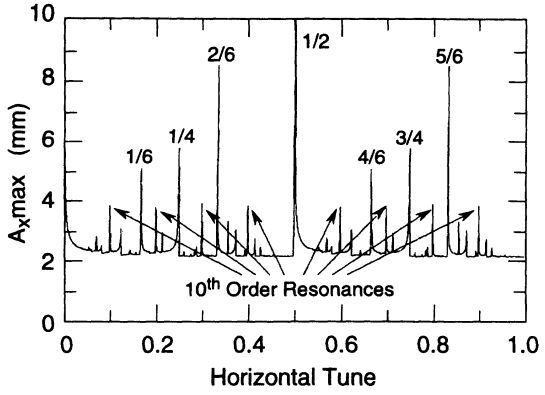

FIG. 3. Maximum horizontal amplitude vs tune for head-on collision. Labels above peaks identify resonances.

nances are the strongest coupling resonances, since they are driven by both of the two largest driving terms.

We can iterate the previous process to obtain the solution of motion. However, this method cannot apply on the resonances because the denominators become zero. The iteration will diverge near the resonances. Therefore the theoretical analysis provides a rough idea of resonance driving strength and simulation was performed to calculate the particle motion.

III. SIMULATION

The simulation described here is aimed to explore the phenomenal difference with and without crossing angle. The results are only expected to make *qualitative* comparison with the theory and experiment, but not quantitative. In the simulation, some physics such as radiation damping and excitation does not change the qualitative results and, therefore, is neglected to enhance the interested physical phenomena.

A simple simulation program similar to Piwinski's work [3] was written to study the crossing-angle collision problem. The simulation program adopts a weak-strong beam-beam interaction model, and consists of only a single beam-beam kick and a linear map for the ring. The beam-beam kick is calculated based on a Padé approach of complex error function [8], and incorporates the crossing-angle collision. Three-dimensional motion is simulated. Particles are launched in six-dimensional phase space with 6σ amplitudes, which are chosen for the same reason as in the theoretical analysis. For convenience of studying resonances, the program scans the horizontal fractional tune from 0 to 1. The maximum amplitude of all particles ever reached during the 1000-turn tracking is recorded as a function of horizontal tune.

A. Head-on collision

The goal of the simulation is to study the nonlinear synchro-betatron coupling due to a beam-beam interaction with a crossing angle. However, even with zero crossing angle, the beam-beam interaction excites many resonances. Therefore, as a baseline, the simulation was done with head-on beams and an uncoupled ring. This result will be used for comparing with crossing-angle collisions to find out which new resonances are excited.

Figure 3 shows the maximum horizontal amplitude of all particles ever reached during the tracking as a function of horizontal tune with the vertical tune being fixed at 12.71. It is easy to identify the spikes in the horizontal amplitude plot. The spikes correspond to the half integer, fourth integer, sixth integer, eighth integer, tenth integer,... resonances, as marked in the picture. Because the beam-beam kick is antisymmetric about the beam axis, only even order resonances are excited.

B. Crossing-angle collision

The results of a simulation with $\Phi = 10$ mrad crossing angle are shown in Fig. 4. Comparing Figs. 3 and 4, it is easy to see many more resonances than in the case of a head-on collision. Some one-dimensional resonances, such as $Q_x = \frac{1}{2}$, $\frac{1}{4}$, and $\frac{1}{6}$, already exist in head-on collision. Besides those resonances, the strongest new resonances are identified as $5Q_x \pm Q_s = \text{integer}$ resonances. The coupling resonance $Q_x \pm Q_s = \text{integer}$ can also be seen

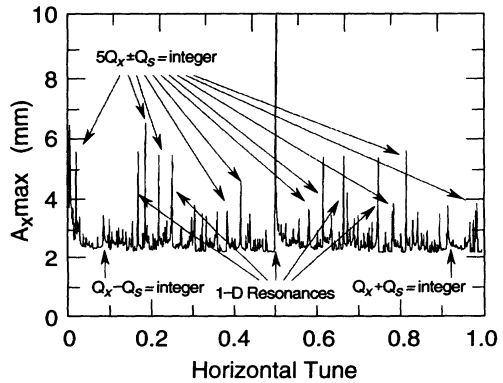

FIG. 4. Maximum horizontal amplitude vs tune for crossing-angle collision ($Q_s = 0.081$).

in this picture. The conclusion supports the theoretical analysis result.

IV. EXPERIMENT

The experiment is designed to observe the $5Q_x+Q_s$ resonance associated with crossing-angle collision, which is predicted by the theory in previous sections. According to the theory, the $5Q_x \pm Q_s$ resonances drive large-amplitude particles to even larger amplitudes, which can result in losing those particles. Therefore one should expect to see a bad lifetime near those resonances.

The experiment is based on the setup of the CESR crossing-angle experiment [4]. CESR has been running with multibunch mode (seven bunches of e^- on seven bunches of e^+). The key point of making multibunch mode possible is to separate bunches around the ring except at the interaction point where the detector is located. In CESR, four electrostatic separators are used to separate electron and positron orbits at parasitic crossing points. As shown in Fig. 5, the orbits (thin lines) are separated at 13 would-be collision points, but are merged between the two south (lower) separators, including the interaction point where the collision takes place. The crossing-angle lattice is essentially a modified version of the normal-operation lattice. The experiment was performed with one bunch on one bunch. A certain amount of antisymmetric voltage is applied to the south separators, which creates antisymmetric orbits about the IP. This is displayed in Fig. 5 as the thick lines. It is easy to see from the picture that the beams will collide at the IP with an angle. The half crossing angle can go up to about ± 2.5 mrad. The crossing angle is limited by the physical aperture at the interaction region (IR) quadrupoles, where the closed orbit is moved to 8.6σ from vacuum chamber.

The procedure of the experiment is similar to the simulation: scan the horizontal tune while the beams collide at an angle, and measure the decay rate (time derivative of the beam current). The weak-strong scenario is reproduced via collisions of a 2-mA beam of electrons and a 10-mA beam of positrons. The tune scan is carried out near the $5Q_x+Q_s=43$ (for $Q_s=0.064$, $Q_x=8.587$) resonance. The reason to choose this resonance is that the crossing-angle lattice working point is close to the resonance (nominal horizontal tune $Q_x=8.57$). It is easy to move the tune to the vicinity of the resonance. In addition, simulation shows that this resonance is in a "clean" area, i.e., there are no other strong resonances near by.

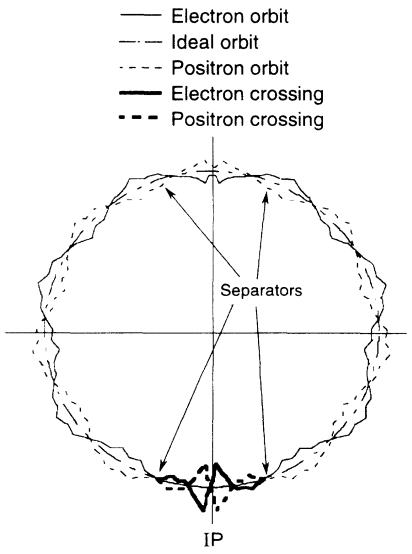

FIG. 5. Diagram of the orbits for the crossing-angle experiment.

A. Measurement of $5Q_x+Q_s$ resonance with and without crossing angle

The experiment described in this section is designed to give a qualitative answer to whether the nonlinear synchro-betatron resonance predicted by the theory exists in practice.

A tune-scan program was used in the measurement. This program automatically changes the tune by changing the strengths of quadrupoles in the arc uniformly. The interaction region quadrupoles are not changed, so that the perturbation to the IR optics is minimized. The tune scan varies tune by only 0.2%. Its effects on optics is unmeasurable. The vertical beam sizes and currents of both beams are measured and recorded after each step of tune change. The vertical beam size is measured by the synchrotron light monitor, but this monitor does not have sensitivity at the large amplitudes studied in this paper. Tunes and tune changing rates were calibrated before each run with the coherent tune shift taken into account. At the beginning of the experiment, the machine was tuned up with two strong beams so that a reasonable luminosity and beam-beam tune shift were achieved. Then, to make a strong-weak collision, the electron beam was removed and a weak electron beam is injected.

The longitudinal frequency has been measured to be 24.5 kHz. Because the CESR revolution frequency f_r is 390 kHz, the synchrotron tune is $Q_s=f_s/f_r=0.0628$.

Before measuring the resonance, the optics is checked by single beam tune scan. One of the important issues is to set chromaticity near zero. This was typically done to ± 0.3. Otherwise, the finite chromaticity introduces tune modulation, which could excite the same resonance $(5Q_x+Q_s)$ with the involvement of sextupole field on single beam.

For comparison, Fig. 6 gives both the simulation results and experimental results. Figure 6(a) shows the simulation results for head-on collisions (solid line) and crossing-angle collisions (dashed line). The plot gives the maximum horizontal amplitude as a function of horizontal tune. It shows that the $5Q_x+Q_s$ resonance appears only when the beams collide at an angle. Figure 6(b) plots the measured results. The data are from two separate measurements: one with the crossing angle turned on (dashed line), and the other one with the angle turned off (solid line). Both measurements employ strong-weak collisions, i.e., 10-mA positron on 2-mA electron. The weak beam (electron) is driven by the reso-

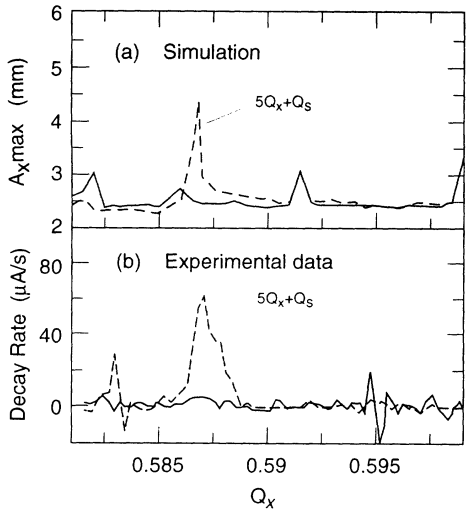

FIG. 6. (a) Simulation result, maximum amplitude vs horizontal tune. (b) Experimental data, decay rate as a function of horizontal tune. Solid lines are the head-on collision data, and dashed lines are the crossing-angle data.

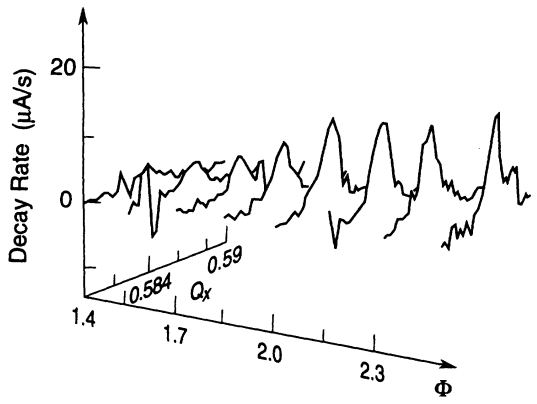

FIG. 7. Tune scans vs different crossing angles.

nance, suffering bad lifetime (or large decay rate). The decay rate is obtained by numerically differentiating the electron current versus time (as the result of differentiation, some jitter in the current measurement creates bipolar spikes, which result in unrealistic negative decay rates). The predicted resonance at $Q_x=0.587$ appears in the data plotted in Fig. 6.

To confirm that what is measured is really the result of crossing-angle collisions, rather than due to the closed orbit effects, a measurement was made with a magnetic orbit distortion. This is the same lattice used to create the crossing angle, except that magnets are used to create an orbit which is very close to one of the crossing-angle orbits. Therefore both beams go through the same magnetic field as in the crossing-angle experiment, but collide head on. In this measurement, we see no resonance excitation, confirming that the resonance is the result of the crossing-angle collision.

B. Resonance strength as a function of crossing angle

The experiment described in this section measures the same resonance by the technique discussed above, as a function of crossing angle. The crossing angle was set to different values and a one-dimensional tune scan was performed to measure the decay rate as a function of tune at each angle. The angle is controlled by the antisymmetric voltage applied to the south separators. Figure 7 gives the measured results. Test runs have indicated that the resonance is not measurable for half crossing angle smaller than 1.4 mrad. Hence detailed measurements took place at larger half crossing angles, up to 2.4 mrad. The picture shows a clear ridge of the decay rate at the $5Q_x+Q_s$ resonance, growing as the crossing angle increases. The result provides the evidence of the consistency of the resonance measurement. It also makes clear that the resonance is directly related to the crossing angle.

An interesting question is how the resonance effect changes with crossing angle. Simulations have been done to investigate the question. The simulation was run with different crossing angles and the maximum amplitude on the resonance was found for each angle. The result is given in Fig. 8(a). From the figure, we see that the maximum amplitude grows rapidly when the half crossing angle is about 1 to 1.2 mrad. After that, the maximum amplitude is almost flat, up to 10 mrad. Figure 8(b) plotted the peak decay rate values of each scan as a function of crossing angle. One can see that the growth of the decay rate peaks is rapid at the beginning, but relatively flat for

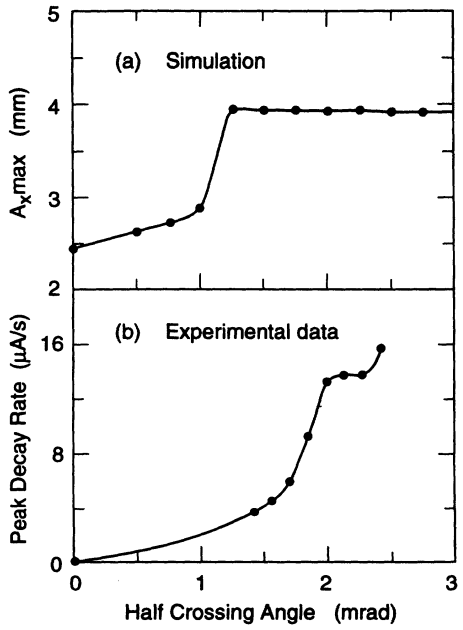

FIG. 8. Resonance strength as a function of crossing angle. (a) Maximum amplitude on the resonance vs crossing angle. (b) Peak decay rate on the resonance vs crossing angle.

large angles.

Comparing Figs. 8(a) and 8(b), one can see some similarity between them. Even though the two plots are not plotting the same quantity, the two quantities reflect the same physical phenomenon. In the two plots, both curves have a rapid rise in the middle, and saturate later. However, there are two obvious differences. First, the experimental data show that the decay rate rises at a larger angle. Second, the last data point in Fig. 8(b) rises again. The differences may be explained as follows: For the first difference, because the radiation damping is not included in the simulation, the particles may be easier to drive to larger amplitudes than in the real situation. In other words, the radiation damping suppresses the amplitude growth that makes the rise of the effect in experiment slower. For the second difference, one can argue that the crossing angle has been pushed to the limit of the physical aperture. The tight physical aperture certainly enhances the decay rate. We know that at the maximum crossing angle there is only 8.6σ physical aperture left at the interaction region quadrupoles. It is obvious that the physical aperture has its influence on the decay rate, and the lifetime is very sensitive to the aperture at such an amplitude. Therefore it is not surprising that a relatively larger decay rate is measured at this angle. For the same reason, the experiment is limited at ± 2.5 mrad crossing angle.

In addition, the 2.4-mrad half crossing angle in the experiment is approximately equal to 0.097 normalized crossing angle. In CESR-B design, the bunch length is significantly reduced. This normalized crossing angle is equivalent to 3.5 mrad in CESR-B

V. CONCLUSION

The study shows a good consistency among analytical results, computer simulations, and experiment on the strongest coupling resonance family excited by the crossing-angle beam-beam interaction. This resonance family, $5Q_x \pm Q_s = \text{integer}$, will result in a bad lifetime in operation. Simulation also shows a saturation of this resonance effect at larger crossing angle. If the saturation is real, it means that good performance might be expected even at the crossing angle required for the B-Factory. However, the experiment does not address the simulation prediction beyond 2.5 mrad.

The observation of the second rise of the decay rate [represented by the last data point in Fig. 8(b)] means either that some other resonance mechanism, as yet unknown, is coming into play, or that it is just an aperture-limiting result. The best way to resolve this is to go to a larger crossing angle. Unfortunately, this is impossible in current CESR, although it may be possible with new, larger aperture quadrupoles near the IP, or with new interaction region optics.

The study is limited in a simplified situation. The couplings, errors, and nonlinearities of the ring and their interference with the beam-beam interaction are not included. The experiment was performed in a limited range of tunes, even though it is near the practical operation point. In B-Factory operation, there may be other resonances excited by the mechanisms that are not considered in this paper.

As mentioned previously, another study [4] investigated the crossing-angle beam-beam problem from the operational point of view. The results show that an e^+e^- collider can operate with a small crossing angle without significant luminosity degradation. The combined results show that the crossing-angle design of the B-Factory might be realistic, even without any compensation, but the $5Q_x \pm Q_s$ resonances have to be avoided in the operation.

ACKNOWLEDGMENTS

The author would like to thank the CESR operations group for their support, D. Rice, D. Rubin, and D. Sagan for help in carrying out the measurements, and M. Tigner for advice and encouragement. More thanks to R. Siemann for his help in improving the paper. Work supported in part by the Department of Energy, Contract No. DE-AC03-76SF00515 and by the National Science Foundation.

[1] A. Piwinski, IEEE Trans. Nucl. Sci. **NS-24**, 1408 (1977).
[2] K. Oide and K. Yokoya, Phys. Rev. A **40**, 315 (1989).
[3] A. Piwinski, SLAC Report No. SLAC-PUB-5430, 1991 (unpublished).
[4] D. Rubin *et al.*, Nucl. Instrum. Methods Phys. Res. A **330**, 12 (1993).
[5] S. Peggs and R. Talman, Annu. Rev. Nucl. Part. Sci. **36**, 287 (1986).
[6] S. Peggs, Ph.D. thesis, Cornell University, 1981.
[7] T. Chen, Ph.D. thesis, Cornell University, 1993.
[8] Y. Okamoto and R. Talman, CESR Report No. CBN 80-13, 1980 (unpublished).